Liquid Crystals
Publication details, including instructions for authors and subscription information:
http://www.informaworld.com/smpp/title~content=t713926090

High birefringence lateral difluoro phenyl tolane liquid crystals

Qiong Song[a]; Sebastian Gauza[a]; Haiqing Xianyu[a]; Shin Tson Wu[a]; Yung-Ming Liao[b]; Chin-Yen Chang[b]; Chain-Shu Hsu[b]
[a] College of Optics and Photonics, University of Central Florida, Orlando, FL, USA [b] Department of Applied Chemistry, National Chiao Tung University, Hsinchu, Taiwan

Online publication date: 11 February 2010

To cite this Article Song, Qiong , Gauza, Sebastian , Xianyu, Haiqing , Wu, Shin Tson , Liao, Yung-Ming , Chang, Chin-Yen and Hsu, Chain-Shu(2010) 'High birefringence lateral difluoro phenyl tolane liquid crystals', Liquid Crystals, 37: 2, 139 — 147
To link to this Article: DOI: 10.1080/02678290903419079
URL: http://dx.doi.org/10.1080/02678290903419079

Liquid Crystals,
Vol. 37, No. 2, February 2010, 139–147

Taylor & Francis
Taylor & Francis Group

High birefringence lateral difluoro phenyl tolane liquid crystals

Qiong Song[a], Sebastian Gauza[a], Haiqing Xianyu[a], Shin Tson Wu[a]*, Yung-Ming Liao[b], Chin-Yen Chang[b] and Chain-Shu Hsu[b]

[a]*College of Optics and Photonics, University of Central Florida, Orlando, FL 32816, USA;* [b]*Department of Applied Chemistry, National Chiao Tung University, Hsinchu, Taiwan*

(Received 24 September 2009; final form 15 October 2009)

Four laterally difluorinated phenyl tolane liquid crystals were synthesised and their physical properties evaluated. These compounds exhibit a fairly small heat fusion enthalpy ($\Delta H \sim 12.56$ kJ mol^{-1}), which is favourable for mixture formulations. For comparison, four lateral difluoro cyclohexane tolane homologues are also studied. We doped 10 wt% of each compound into a commercial negative mixture N1 and measured the birefringence, visco-elastic coefficient and figure of merit. Birefringence varies very little between homologues, but the visco-elastic coefficient increases as alkyl chain length increases. The refractive indices of these guest–host mixtures at 1550 nm are also measured.

Keywords: high birefringence; negative dielectric anisotropy; liquid crystals

1. Introduction

High birefringence (Δn) and low-viscosity nematic liquid crystals (LCs) are useful electro-optic media for laser beam steering, telecommunications, reflective displays and adaptive lenses [1–5]. In the past decade, considerable attention has been paid to the synthesis of tolane-based LCs because of their high birefringence [6, 7]. Several molecular structures with high Δn values, e.g. diphenyl-diacetylene [8–10], biphenyl-tolane [11–14], bistolane [15–18], naphthalene tolanes [19], naphthyl-bistolanes [20] and thiophenylacetylene [21, 22], have been investigated. However, three major shortcomings of these highly conjugated LC compounds are found: (1) high melting point; (2) high viscosity; and (3) inadequate photo- and thermal-stabilities [23]. For instance, if the temperature is increased to above 270°C an irreversible polymerisation process would occur, as marked by a colour change to dark brown. Many efforts have been taken to lower the melting temperature [24–30].

In this paper, we report the physical properties of following lateral difluoro compounds, Structures (I) and (II):

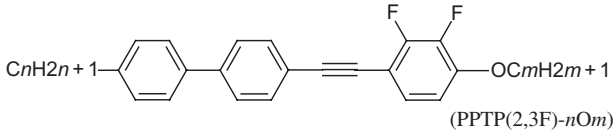

(PPTP(2,3F)-*n*O*m*)

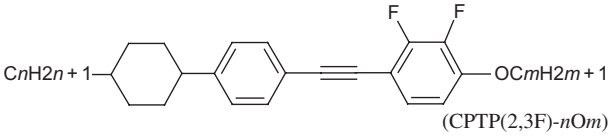

(CPTP(2,3F)-*n*O*m*)

The tolane unit, comprising of two phenyl rings linked by a carbon–carbon triple bond, forms the main part of the rigid core of the molecules and defines the principal molecular axis [31]. The unsaturated phenyl ring is rich in π-electrons. Thus, these rings are particularly desirable for elongating π-electron conjugation through the rod-like molecule and increasing the polarisability along the principal molecular axis. The triple bond is an effective π-electron acceptor. In addition, its contribution to viscosity is not so significant. The oxygen atom in the alkoxy chain elongates the π-electron conjugation, but it also increases the visco-elastic coefficient and melting temperature.

In each structure, four homologues are selected in order to study their physical properties. These compounds have a relatively high melting point. Therefore, it is inconvenient to measure their properties at elevated temperatures. Instead, we doped 10 wt% of each compound into a commercial negative dielectric anisotropy ($\Delta\varepsilon$) mixture and measured the dielectric anisotropy, birefringence, visco-elastic coefficient and figure-of-merit (*FoM*) of the guest–host mixtures. For a compound with a high melting point or large heat fusion enthalpy, it is important to make certain whether the guest is dissolved into the host completely. Otherwise, the measured results will not be accurate. We usually leave the prepared guest–host mixtures for one night to see if there is any precipitation. In order to improve the solubility of high birefringence compounds, we choose a host mixture with a low melting point.

In order to measure the birefringence more accurately, we also used an Abbe refractrometer to measure the individual refractive indices (n_e and n_o). The

*Corresponding author. Email: swu@mail.ucf.edu

ISSN 0267-8292 print/ISSN 1366-5855 online

DOI: 10.1080/02678290903419079
http://www.informaworld.com

measured wavelength dependent n_e and n_o results fit well with the extended Cauchy model [32, 33].

Finally, we used HyperChem (v.7) single personal computer (PC) software to simulate the dipole moment and mean polarisability of these compounds. The results were used to compare with the extrapolated dielectric anisotropy and birefringence of these compounds. Since the simulation is based on a single molecule calculated '*in vacuo*' to its possibly lowest energy gradient, which suggests most possible configuration of the molecule, the result can qualitatively explain the observed differences between phenyl tolane and cyclohexane tolane, but it does not agree exactly with each homologue in the same category.

2. Compound synthesis

Both series of PPTP(2,3F)-*n*O*m* and CPTP(2,3F)-*n*O*m* were prepared by Cadiot-Chodkiewicz coupling of 1-(4-alkoxyl-2,3-difluorophenyl) acetylene with 4-alkyl-4'-iodobiphenyl and 4-alkylcyclohexyl-1-iodobenzene, respectively [34]. The intermediate compounds 1-(4-alkoxyl-2,3-difluorophenyl)acetylene, 4-alkyl-4'-iodobiphenyl and 4-alkylcyclohexyl-1-iodobenzene were prepared according to the synthetic procedures reported by the National Chiao Tung University (NCTU) group [34, 35]. All of the synthesised LC compounds were purified several times by column chromatography until their purities (checked by high-performance liquid chromatography (HPLC)) were higher than 99.0%.

2.1 Synthesis of CPTP(2,3F)-4O2

Compound 4-butylcyclohexyl-1-iodobenzene (1.709 g, 4.99 mmol), $Pd(PPh_3)_2Cl_2$ (0.116 g, 0.076 mmol), triphenylphosphine (0.105 g, 0.40 mmol), CuI (0.019 g, 0.100 mmol) and dry triethylamine (50 mL) were mixed and stirred at room temperature for 30 min under nitrogen. A solution of 1-(4-ethoxyl-2,3-difluorophenyl) acetylene (1 g, 4.99 mmol) dissolved in 10 mL of triethylamime was added dropwise and the mixture stirred at 60°C for 24 h. After cooling to room temperature, the mixture was filtered and the filtrate concentrated *in vacuo* to remove the triethylamine. The crude product was dissolved in diethyl ether and extracted with aqueous ammonium chloride solution. The organic phase was then washed with saturated aqueous NaCl and dried over $MgSO_4$. The crude product isolated by evaporating the solvent was purified by column chromatography using ethyl acetate/*n*-hexane = 1/20 as the eluant to give a white solid; yield 0.47 g (24%); purity 99.5%. ^{1}H nuclear magnetic resonance (NMR) ($CDCl_3$, trimethylsilyl (TMS), 300 MHz), δ 7.38–7.36 (d, 2H, J = 9 Hz, aromatic protons), 7.15–7.05 (m, 3H, aromatic protons), 6.63–6.57 (m, 1H, aromatic protons), 4.09–4.02 (q, 2H, J = 6.6 Hz, –OC<u>H</u>$_2$CH$_3$), 2.43–0.76 (m, 19H, –C$_4$<u>H</u>$_9$ and cyclohexyl C$_6$<u>H</u>$_{10}$); ^{13}CNMR ($CDCl_3$, TMS, 75 MHz): 153.59, 153.43, 150.25, 148.88, 143.14, 139.86, 131.78, 127.26, 127.21, 127.14, 120.35, 109.29, 106.16, 105.98, 98.82, 94.25, 81.25, 65.61, 44.83, 37.48, 37.30, 34.35, 33.73, 29.45, 23.24, 14.89, 14.37.; mass spectroscopy (MS) m/z (M^+) 396; Calculated for $C_{26}H_{30}OF_2$: C, 78.76; H, 7.63. found: C, 78.77; H, 7.91.

2.2 Synthesis of PPTP(2,3F)-4O3

Compound 4-butyl-4'-iodobiphenyl (3.765 g, 11.2 mmol), $Pd(PPh_3)_2Cl_2$ (1.6 g, 2.2 mmol), triphenylphosphine (0.6 g, 2.2 mmol), CuI (0.4 g, 2.2 mmol) and dry triethylamine (60 mL) were mixed and stirred at room temperature for 30 min under nitrogen. A solution of 1-(4-ethoxyl-2,3-difluorophenyl) acetylene (3 g, 11.2 mmol) dissolved in 20 mL of triethylamime was added dropwise and the mixture stirred at 60°C for 24 h. After cooling to room temperature, the mixture was filtered and the filtrate concentrated *in vacuo* to remove the triethylamine. The crude product was dissolved in diethyl ether and extracted with aqueous ammonium chloride solution. The organic phase was then washed with saturated aqueous NaCl and dried over $MgSO_4$. The crude product isolated by evaporating the solvent was purified by column chromatography using *n*-hexane as the eluant to give a white solid; yield 2.62 g (60%); purity 99.3%. ^{1}H NMR($CDCl_3$, TMS, 300 MHz): δ 7.57–7.49 (m, 6H, aromatic protons), 7.26–7.24 (d, 2H, J = 6 Hz, aromatic protons), 7.21–7.15 (m, 1H, aromatic proton), 6.72–6.66 (m, 1H, aromatic proton), 4.04–3.99 (t, 2H, J = 6.6 Hz, –Ph–OC<u>H</u>$_2$–CH$_2$–CH$_3$), 2.66–2.13 (t, 2H, J = 6 Hz, –Ph–C<u>H</u>$_2$–CH$_2$–CH$_2$–CH$_3$), 1.91–1.79 (m, 2H, –Ph–OCH$_2$–CH$_2$ –C<u>H</u>$_3$), 1.67–1.57 (m, 2H, –Ph–CH$_2$–C<u>H</u>$_2$–CH$_2$–CH$_3$), 1.46–1.31 (m, 2H, –Ph–CH$_2$–CH$_2$–C<u>H</u>$_2$ C–H$_3$), 1.09–1.04 (t, 3H, J =7 Hz, –Ph–OCH$_2$–CH$_2$–C<u>H</u>$_3$), 0.95–0.90 (t, 3H, J =7Hz, –Ph–CH$_2$–CH$_2$–CH$_2$–C<u>H</u>$_3$).; ^{13}C NMR($CDCl_3$, TMS, 75 MHz): δ 153.3, 150.9, 142.8, 141.9, 137.4, 132.9, 128.9, 127.1, 126.8, 121.4, 109.0, 103.1, 92.5, 66.2, 35.3, 33.6, 29.7, 22.4, 14.0.; high-resolution mass spectroscopy (HRMS) of $C_{27}H_{26}OF_2$: calculated: 404.1952, found: 404.1953.

3. Phase transitions

Differential Scanning Calorimetry (DSC, TA Instrument Model Q-100) was used to determine the phase transition temperatures. The results were

obtained from 3–6 mg samples in the heating and cooling cycles at a scanning rate of 2°C min^{-1}. According to the Schroder–Van Laar equation, both low melting temperature and low heat fusion enthalpy play equally important roles in reducing the melting temperature of a eutectic mixture. A low melting temperature and a high clearing point are critical for practical device applications. Normally, the desirable nematic range of a LC mixture is from –40 to +85°C.

As shown in Table 1, Compound PPTP (2,3F)-4O3 has a low enthalpy (~12.56 kJ mol^{-1}), which is favourable for making a eutectic mixture. However, its melting point is still relatively high (~110°C), which on the other hand limits its solubility to a mixture. The homologue PPTP(2,3F)-6O4 exhibits a smectic phase because the tendency to form a smectic phase increases as the alkyl chain length increases. To suppress the smectic phase and reduce the melting point, we replace the left phenyl ring with a cyclohexane ring, as Structure (II) shows. From Table 1, we find that Structure (II) has a much lower melting point than Structure (I). The lower melting point is mainly attributed to the non-planar structure of cyclohexane ring, in addition to that caused by the lateral difluoro groups. Because of the lower melting point, the solubility of Structure (II) is better than that of Structure (I), except that its Δn is lower.

4. Electro-optical properties

The Abbe refractrometer is a useful instrument for measuring the refractive indices of LC materials. However, to characterise other physical properties like birefringence, visco-elastic coefficient, and *FoM*, we used electro-optic method [36–38]. Birefringence was obtained through measuring the phase retardation of 7 μm homeotropic cells (pretilt angle ~87°) using a He–Ne laser (λ = 633 nm) [36]. At a given temperature, the phase retardation is related to cell gap d, birefringence Δn, and wavelength λ as

$$\delta = 2\pi d\Delta n/\lambda. \quad (1)$$

For a vertically aligned cell, each compound's performance was compared based on the *FoM* defined as [38]

$$FoM = K_{33}(\Delta n)^2/\gamma_1, \quad (2)$$

where K_{33} is the bend elastic constant and γ_1 is the rotational viscosity. Temperature has a great influence on the LC device performance. As the temperature increases, birefringence, dielectric anisotropy, elastic constants and viscosity all decrease, but at different rates. It is important to know the exact behaviour of the guest–host mixture throughout the entire operation temperature range. Therefore, in the following sections we report each parameter under different temperatures.

4.1 *Dielectric anisotropy*

From mean-field theory [39], the dielectric constants of a LC compound are governed by the dipole moment and its relative position with respect to the principal molecular axis. Negative dielectric anisotropy ($\Delta\varepsilon < 0$) originates from the lateral difluoro group. The dielectric constants of a LC affect the operating voltage. The threshold voltage V_{th} of a homeotropic cell is related to the dielectric anisotropy and bend elastic constant K_{33} as follows:

$$V_{th} = \pi\sqrt{\frac{K_{33}}{\varepsilon_o\Delta\varepsilon}}. \quad (3)$$

Thus, low-threshold voltage can be obtained by either enhancing the dielectric anisotropy, reducing the elastic constant, or a combination of both.

The dielectric anisotropy of Structures (I) and (II) was measured based on 10 wt% guest doped in N1 host and the results extrapolated. An inductance, capacitance, resistance (LCR) Hitester (Model HIOKI

Table 1. Phase transitions of the PPTP and CPTP homologues. MW: Molecular weight, K: Crystalline, Sm: Smectic, and N: Nematic phase. ΔH: Heat fusion enthalpy.

Compounds	MW (g)	K→Sm (°C)	Sm →N (°C)	N →I (°C)	ΔH (kJ mol^{-1})
PPTP(2,3F)-4O3	404	109.4		256.7	13.25
PPTP(2,3F)-5O4	432	110.2		202.7	12.51
PPTP(2,3F)-6O3	432	103.4		212.0	13.13
PPTP(2,3F)-6O4	446	105.4	129.1	200.4	10.26
CPTP(2,3F)-3O2	380	84.0		228.0	25.12
CPTP(2,3F)-4O2	396	70.3		211.4	26.89
CPTP(2,3F)-5O2	408	73.0		217.0	27.21
CPTP(2,3F)-6O2	424	73.8		199.2	30.09

Table 2. Extrapolated Δε of the PPTP and CPTP homologues.

	Δε at 22°C
PPTP(2,3F)-4O3*	–4.06
PPTP(2,3F)-5O4	–4.37
PPTP(2,3F)-6O3	–4.00
PPTP(2,3F)-6O4	–3.13
CPTP(2,3F)-4O2	–6.25
CPTP(2,3F)-6O2	–4.05
CPTP(2,3F)-3O2	–6.35
CPTP(2,3F)-5O2	–5.65

*The value of PPTP (2,3F)-4O3 is extrapolated from 10 wt% doped in MLC-6608.

3532-50) was used to measure the capacitance of the homogeneous and homeotropic cells with or without LC mixtures. Dielectric anisotropy represents the difference between the parallel and the perpendicular components of the dielectric constant. The measured results are shown in Table 2. The 10 wt% PPTP(2,3F)-4O3 has a solubility problem in N1, so we choose MLC-6608 as the host. The lateral difluoro PPTP and CPTP series have dielectric anisotropy of about –4 and –6, respectively. Previously, a high birefringence biphenyl tolane with $\Delta\varepsilon \sim -8$ was reported [12]. Our value is roughly one half of this, because Structures (I) and (II) have only one pair of difluoro groups, while the reported compound has two pairs. The tolane structure is pretty much co-planar, as a result, more lateral dipoles would lead to a larger negative Δε.

4.2 *Birefringence*

The temperature dependent birefringence of a LC can be described as follows:

$$\Delta n = \Delta n_o S, \tag{4}$$

$$S \approx (1 - T/T_c)^{\beta}, \tag{5}$$

where Δn_o is the birefringence at $T = 0$ K, S is the order parameter, β is a material constant, and T_c is the clearing temperature of the LC. Δn_o and β were obtained by fitting the experimental data using Equations (4) and (5).

Figures 1(a) and (b) shows the temperature dependent birefringence for the N1 host doped with four homologues of Structures (I) and (II), respectively. In the whole temperature range from room temperature to T_c, the PPTP(2,3F) series shows a ~17% higher birefringence than N1, while the CPTP(2,3F) series is ~13%. This is because both Structures (I) and (II) have a longer conjugation than the host mixture.

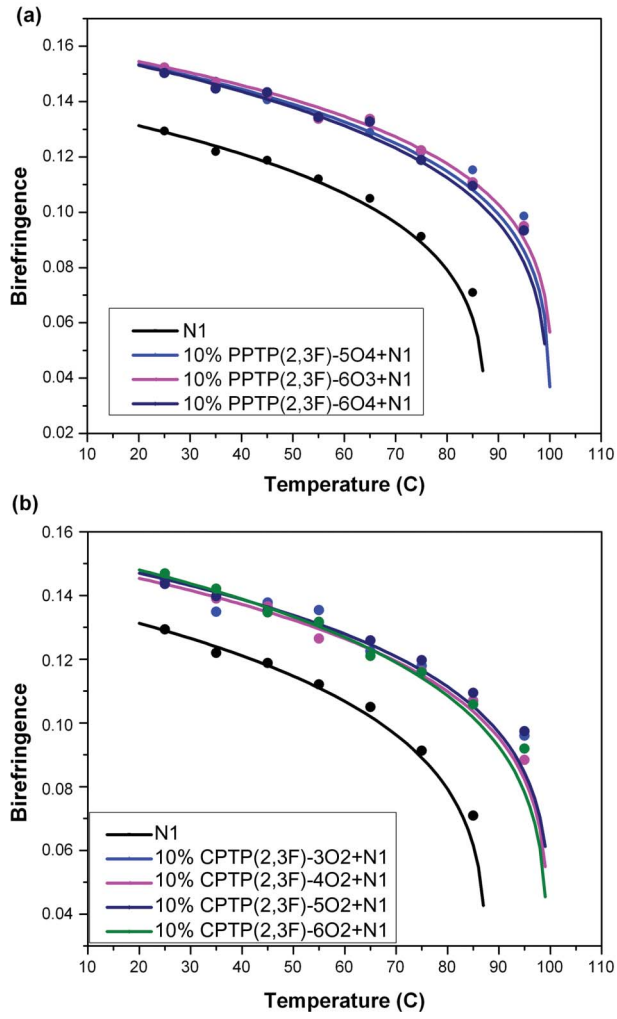

Figure 1. Measured birefringence of N1 host and four (a) PPTP and (b) CPTP homologues in N1 host. The dots are experimental data and the lines are fitting results.

PPTP(2,3F)-4O3 has a solubility problem in N1, so we do not include its data in the figures.

4.3 *Visco-elastic coefficient*

The rotational viscosity is dependent on the activation energy, the molecular moment of inertia (including molecular shape and mass) and the temperature [37]. Thus, a linearly conjugated LC is favoured for its large optical anisotropy and relatively low rotational viscosity.

From Figure 2, we can see that even if we only dope 10 wt% of each compound in N1, the alkyl chain effect on the visco-elastic coefficient is very obvious: the longer the alkyl chain, the larger the visco-elastic coefficient [40]. In the PPTP series, the homologues -5O4, -6O3 and -6O4 cause the visco-elastic coefficient of N1 to increase by 40.5%, 44.6%, and 54.5%, respectively. For the CPTP series, the homologues -3O2, -4O2, -5O2

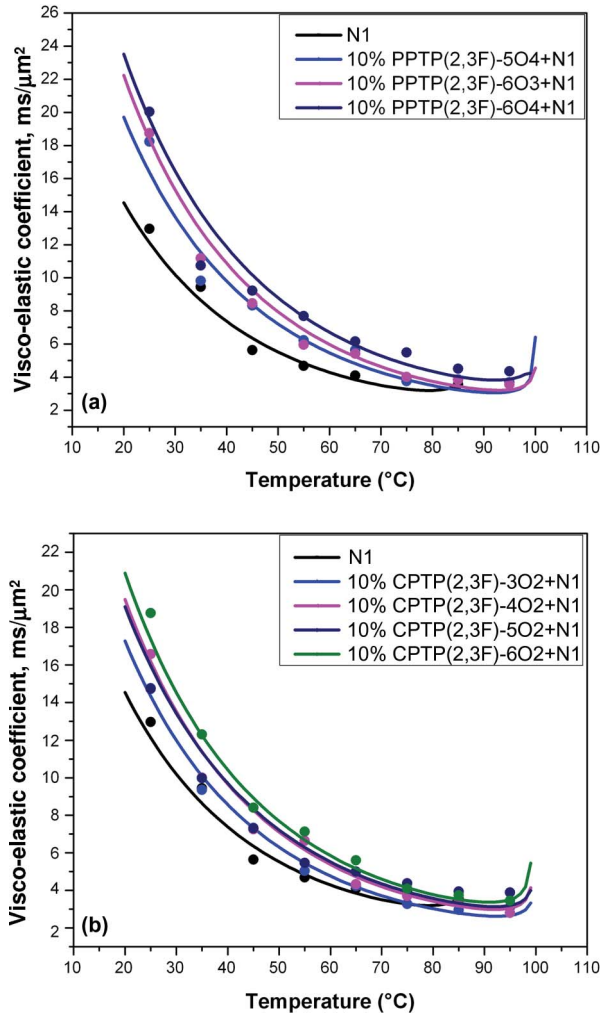

Figure 2. Visco-elastic coefficient of four (a) PPTP and (b) CPTP compounds doped in N1 host. The dots are experimental data and the lines are fitting results.

and -6O2 boost the visco-elastic coefficient of N1 by 13.9%, 27.8%, 29.0% and 44.7%, respectively.

4.4 *Figure of merit*

Using Equation (2) and knowing that $K_{33} \sim S^2$ and $\gamma_1 \sim S \cdot \exp(E/kT)$, the *FoM* can be expressed as follows [38]:

$$FoM = a\Delta n_o^2 (1 - T/T_c)^{3\beta} \exp(-E/kT). \quad (6)$$

In Equation (6), a is the proportionality constant, k is the Boltzmann constant and E is the activation energy of molecular rotation. The *FoM* is commonly used to compare the performance of a LC compound or mixture because it is independent of the cell gap employed.

Figure 3(a) and (b) shows the temperature dependent *FoM* of the PPTP and CPTP compounds doped in the N1 host. Birefringence varies very little within the same homologues series, while the visco-elastic coefficient becomes larger as the alkyl chain length increases, so the *FoM* is mainly governed by the visco-elastic coefficient. PPTP(2,3F)-5O4 and PPTP(2,3F)-6O3 have a similar *FoM*, which is higher than that of N1, while PPTP(2,3F)-6O4 improves the *FoM* of N1 only at high temperatures. Among the CPTP(2,3F) series, CPTP(2,3F)-3O2 has the largest *FoM* because it has the lowest visco-elastic coefficient, followed by CPTP (2,3F)-4O2 and CPTP(2,3F)-5O2: and CPTP(2,3F)-6O2 has the smallest *FoM*. As shown in Figures 1 and 2, the alkyl chain length makes a more pronounced effect on the visco-elastic coefficient than on

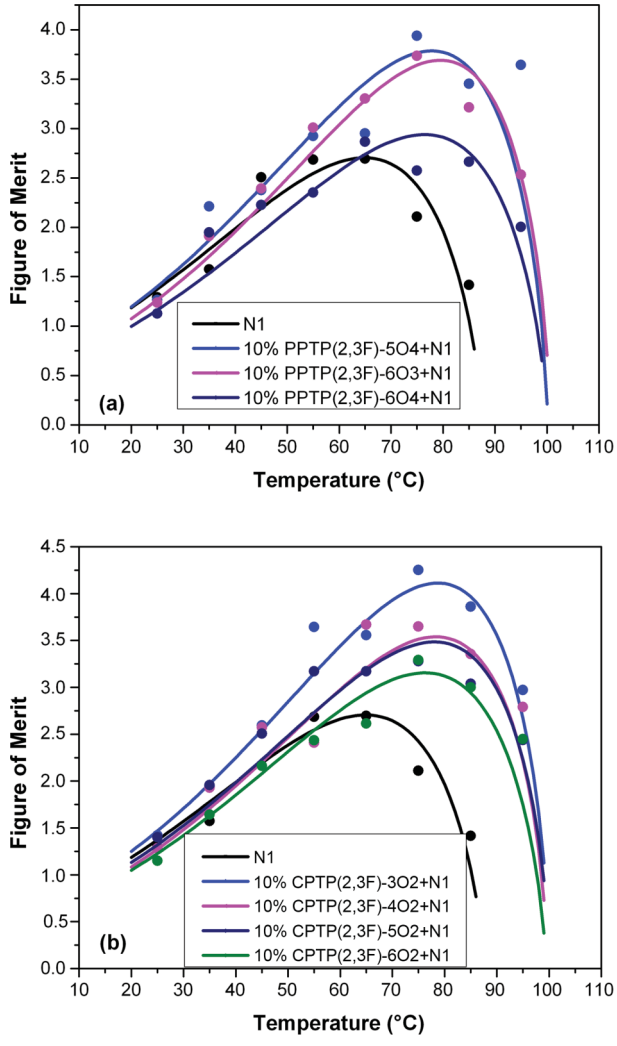

Figure 3. Measured *FoM* of N1 and (a) three PPTP homologues and (b) four CPTP homologues in the N1 host. The dots are experimental data and the lines are fitting results.

birefringence for the same rigid core structure compared. Thus, a shorter alkyl chain is preferred from a high *FoM* standpoint. However, the trade-off is the higher melting point.

5. Birefringence measurements

We used a multi-wavelength Abbe refractrometer (Atago: DR-M4) to measure the LC refractive indices at six wavelengths ($\lambda = 450$, 486, 546, 589, 633 and 656 nm) by changing the colour filters. We used a 0.294% hexadecyletri-methyle-ammonium bromide (HMAB)+ methanol solution to align the LC molecules perpendicular to the surfaces of the prisms. The LC refractive indices (n_e and n_o) decrease as the wavelength increases, and then saturate in the infrared (IR) region. It is found that the LC birefringence drops ~10–20% as the wavelength increases from the visible to the IR.

For the compound with a high melting point, it is inconvenient to measure its physical properties at elevated temperatures. Instead, we extrapolate its properties by doping 10 wt% of each compound to a negative $\Delta\varepsilon$ LC host, designated as N1. The physical properties of N1 are listed in Table 3. N1 has a modest birefringence, a fairly large negative dielectric anisotropy ($\Delta\varepsilon \sim -5$) and a low melting point (<–30°C), which helps to improve the solubility of the guest compounds. The extrapolated birefringence values are listed in Table 4.

Table 3. Physical properties of N1 host.

K→N (°C)	Clearing point (°C)	Viscosity (mm^2 s^{-1}, 20°C)	Δn (589 nm, 20°C)	$\Delta\varepsilon$ (1 kHz, 25°C)
<–30	85	35	0.134	–5.1

Table 4. Extrapolated Δn of the PPTP and CPTP compounds at $\lambda = 633$ nm and 25°C.

	Δn
N1	0.1293
PPTP(2,3F)-4O3*	0.3818
PPTP(2,3F)-6O3	0.3633
PPTP(2,3F)-6O4	0.3478
PPTP(2,3F)-5O4	0.3590
CPTP(2,3F)-3O2	0.2988
CPTP(2,3F)-4O2	0.2763
CPTP(2,3F)-5O2	0.2863
CPTP(2,3F)-6O2	0.2676

*The value of PPTP (2,3F)-4O3 is extrapolated from 8 wt% doped in MLC-6608.

The Δn of a LC compound is mainly determined by the electron conjugation, differential oscillator strength and order parameter. If we use the single-band model, the birefringence dispersion of a uniaxial LC can be expressed as [41]

$$\Delta n = G(T)\frac{\lambda^2\lambda^{*2}}{\lambda^2 - \lambda^{*2}}, \tag{7}$$

where G is a proportionality constant, which is related to the molecular packing density, order parameter (S) and the differential oscillator strength, and λ^* is the mean resonance wavelength, which depends on the molecular conjugation. In the same LC homologues, molecules with a shorter side chain may exhibit a larger Δn owing to the conformational effect. This equation explains the reason why the comparison of birefringence for different LC materials has to be made at the same reduced temperature and same wavelength.

Figure 4 shows the measured absorption spectrum of PPTP (2,3F)-4O3 in a cyclohexane solvent. The LC concentration is 2×10^{-4} mol l^{-1} and the cell gap of the ultraviolet (UV) quartz cuvette is 1 mm. There are two absorption bands centred at $\lambda_2 \sim 200$ nm and $\lambda_3 \sim 310$ nm. From the three-band model [42], the long λ_3 leads to a high birefringence. We also measured the clearing point of 10 wt% doped N1; the clearing points are very close to $T_c = 100$°C. So, the possible reason for the birefringence difference among the homologues is from the molar ratio difference and the alkyl chain effect.

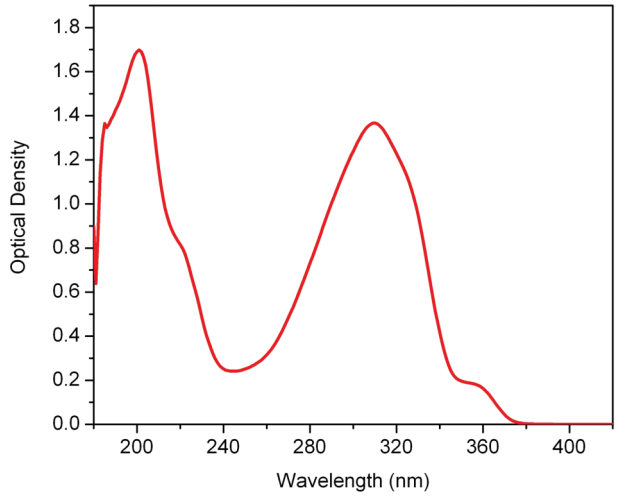

Figure 4. The measured UV absorption spectrum of PPTP(2,3F)-4O3. The compound is dissolved in cyclohexane with 2×10^{-4} mol l^{-1} concentration and 1 mm cell gap.

Within the same homologues, compound PPTP(2,3F)-4O3 has the highest birefringence ($\Delta n \sim 0.382$) and PPTP(2,3F)-6O4 has the smallest birefringence (~ 0.348). The birefringence difference is 9.8%. The molecular weight difference between these two homologues is 10.4%, which is very close. Next, we compare PPTP(2,3F)-5O4 with PPTP(2,3F)-6O3 in which the alkyl chain length and molecular weight are the same. Their birefringence difference is only 1.2%, which is within the experimental error. The birefringence difference between PPTP(2,3F)-6O4 and PPTP(2,3F)-5O4 is 3.2%, which is also consistent. Next, let us look at the CPTP series. The extrapolated birefringence is around 0.28; a small variation among the homologues is found.

The wavelength effect on LC refractive indices is important for the design of direct-view displays and photonic devices. Wavelength-dependent refractive indices of N1 and N1 doped with 10 wt% PPTP and CPTP compounds at 25°C are shown in Figures 5 and 6, respectively. The filled circles, triangles and squares represent the experimental data for n_e and n_o of each mixture. The dashed lines are fittings by using the extended three-coefficient Cauchy model [32, 33] as follows:

$$n_{e,o} = A_{e,0} + \frac{B_{e,o}}{\lambda^2} + \frac{C_{e,o}}{\lambda^4}. \tag{8}$$

The fitting parameters are listed in Table 5. Some n_o values are beyond the range of our Abbe refractrometer, thus, we have only measured at four wavelengths. Therefore, its fitting is not as accurate as n_e. From the fitting parameters, we can estimate the birefringence in the IR region. As Table 5 shows, the average

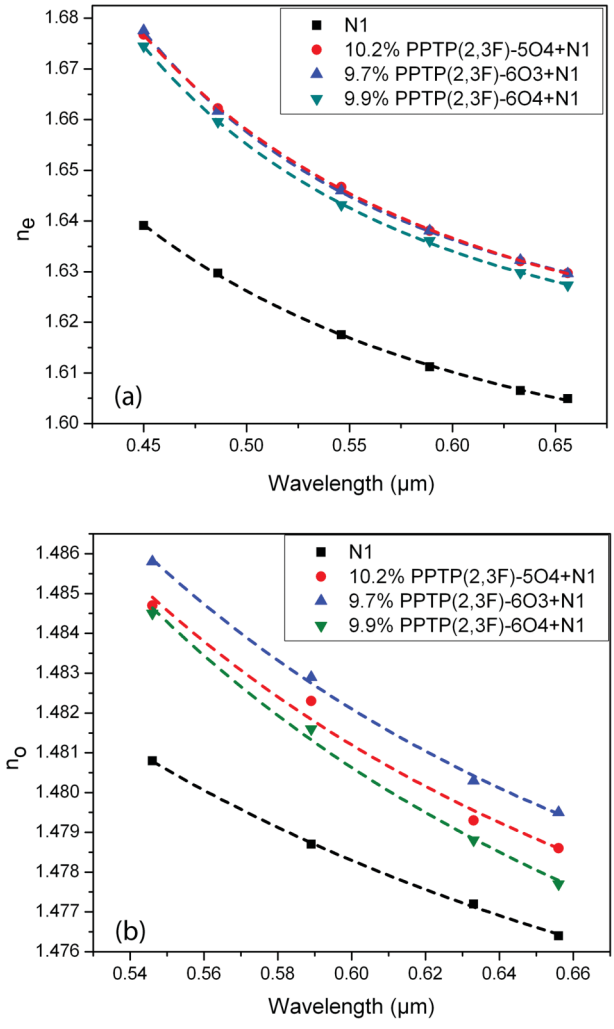

Figure 5. Wavelength dependent (a) n_e and (b) n_o of four PPTP(2,3F) homologues in the N1 host. The dots are measured data and the dashed lines are fittings with Equation (8).

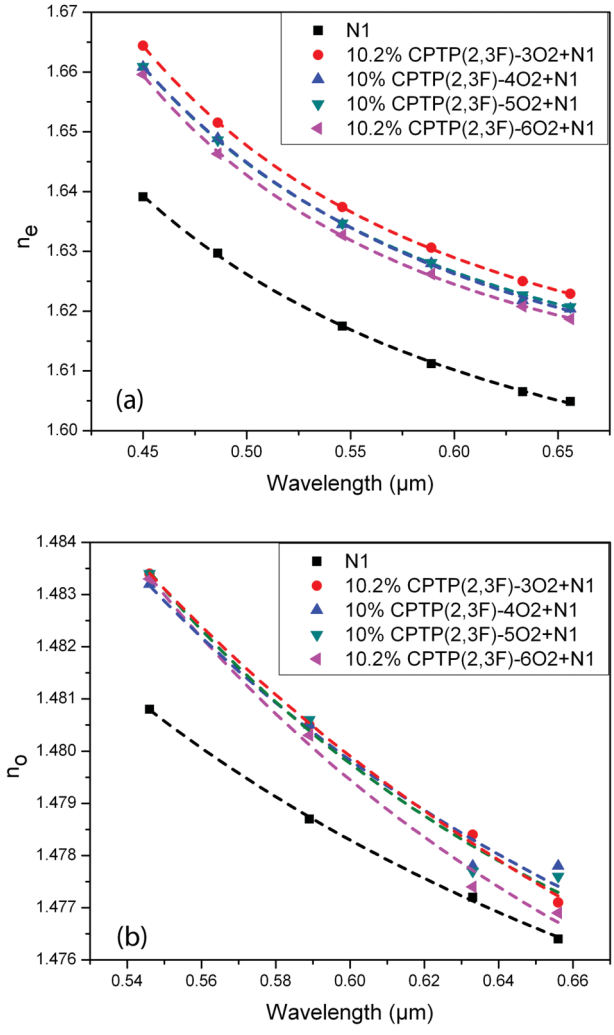

Figure 6. Wavelength dependent (a) n_e and (b) n_o of four CPTP(2,3F) homologues in the N1 host. The dots are measured data and the dashed lines are fittings with Equation (8).

Table 5. Fitting parameters of the wavelength dependent n_e and n_o of the eight guest–host mixtures studied.

	Δn	n_e			n_o		
	($\lambda = 1.55$ μm)	A_e	B_e	C_e	A_o	B_o	C_o
N1	0.1134	1.5787	0.01013	0.00043	1.4684	0.00293	0.00023
10.25% PPTP(FF)-5O4+N1	0.1443	1.6009	0.00966	0.00115	1.4647	0.00584	0.00005
9.7% PPTP(FF)-6O3+N1	0.1414	1.6078	0.00540	0.00176	1.4653	0.00593	0.00005
9.93% PPTP(FF)-6O4+N1	0.1454	1.6035	0.00667	0.00156	1.4641	0.00534	0.00023
10.2% CPTP(FF)-3O2+N1	0.1376	1.5991	0.00759	0.00114	1.4645	0.00509	0.00016
10% CPTP(FF)-4O2+N1	0.1223	1.5937	0.00928	0.00087	1.4679	0.00304	0.00045
10% CPTP(FF)-5O2+N1	0.1279	1.5973	0.00755	0.00108	1.4704	0.00092	0.00089
10.2% CPTP(FF)-6O2+N1	0.1326	1.5984	0.00559	0.00137	1.4673	0.00240	0.00071

birefringence at $\lambda = 1.55$ μm of 10 wt% Structures (I) and (II) in the N1 host is 0.144 and 0.125, respectively. Compared to the birefringence of N1 at 1.55 μm, the ~10 wt % PPTP and CPTP guests enhance the Δn by 26.9% and 10.3%, respectively.

6. Molecular modelling of phenyl tolane compounds

We used HyperChem (v.7) single PC software to calculate the dipole moment and the mean polarisability of phenyl/cyclohexane tolane compounds. Table 6 lists the simulation results. PPTP (2,3F)-4O3 contains two laterally substituted fluoro groups into the (2,3) phenyl ring's positions. The electronegativity of fluorine is known to be 4 and will always pull the electrons away from the atom, which has a lower electronegativity value. The large dipole moment calculated for phenyl/cyclohexane is a natural consequence of the electron's pull effect. The classical Lorentz–Lorenz equation [43] correlates the refractive index of an isotropic media with molecular polarisability in the optical frequencies. We calculated the mean polarisability of the eight compounds studied and found without surprise that compounds with a longer π-electron conjugation show a higher polarisability and birefringence [44, 45].

Table 6. Simulated dipole moment and molecular polarisability of the eight phenyl tolane compounds studied.

	Dipole moment (Debye)	Mean polarisability (a.u.)
PPTP(2,3F)-4O3	3.718	287.8
PPTP(2,3F)-5O4	3.696	304.4
PPTP(2,3F)-6O3	3.715	304.4
PPTP(2,3F)-6O4	3.784	312.9
CPTP(2,3F)-4O2	3.814	262.3
CPTP(2,3F)-6O2	3.819	278.4
CPTP(2,3F)-3O2	3.815	254.1
CPTP(2,3F)-5O2	3.819	270.4

7. Conclusion

We have synthesised and studied two series of high birefringence negative Δε LC compounds: (2,3) lateral difluoro PPTP and CPTP. These compounds exhibit a high birefringence and modest negative dielectric anisotropy. Their visco-elastic coefficient and *FoM* is dependent on the alkyl chain length. These negative LC compounds are intended to enhance the birefringence of dual-frequency LC mixtures for IR applications.

Acknowledgement

The authors are indebted to the Air Force Office of Scientific Research (AFOSR) for financial support under Contract No. FA95550-09-1-0170.

References

[1] McManamon, P.F.; Dorschner, T.A.; Corkum, D.L.; Friedman, L.; Hobbs, D.S.; Holz, M.; Liberman, S.; Nguyen, H.Q.; Resler, D.P.; Sharp, R.C.; Watson, E.A. *Proc. IEEE* **1996**, *84*, 268–298.
[2] Wu, S.T.; Yang, D.K. *Reflective Liquid Crystal Displays*; Wiley: New York, 2001.
[3] Drzaic, P.S. *Liquid Crystal Dispersions*; World Scientific: Singapore; River Edge, NJ, 1995.
[4] Sutherland, R.L.; Tondiglia, V.P.; Natarajan, L.V. *Appl. Phys. Lett.* **1994**, *64*, 1074–1076.
[5] Ren, H.W.; Wu, S.T. *Appl. Phys. Lett.* **2003**, *82*, 22–24.
[6] Gray, G.W.; Mosley, A. *Mol. Cryst. Liq. Cryst.* **1976**, *37*, 213–231.
[7] Wu, S.T.; Cox, R.J. *J. Appl. Phys.* **1988**, *64*, 821–826.
[8] Grant, B. *Mol. Cryst. Liq. Cryst.* **1978**, *48*, 175–182.
[9] Wu, S.T.; Margerum, J.D.; Meng, B.H.; Dalton, L.R.; Hsu, C.S.; Lung, S.H. *Appl. Phys. Lett.* **1992**, *61*, 630–632.
[10] Wu, S.T.; Hsu, C.S.; Chen, Y.N.; Wang, S.R. *Appl. Phys. Lett.* **1992**, *61*, 2275–2277.
[11] Liao, Y.M.; Janarthanan, N.; Hsu, C.S.; Gauza, S.; Wu, S.T. *Liq. Cryst.* **2006**, *33*, 1199–1206.
[12] Xianyu, H.Q.; Gauza, S.; Song, Q.; Wu, S.T. *Liq. Cryst.* **2007**, *34*, 1473–1478.

[13] Wu, S.T.; Hsu, C.S.; Chen, J.M. *Mol. Cryst. Liq. Cryst.* **1997**, *304*, 441–445.
[14] Dziaduszek, J.; Dabrowski, R.; Ziółek, A.; Gauza, S.; Wu, S.T. *Opto-Electron. Rev.* **2009**, *17*, 20–24.
[15] Wu, S.T.; Hsu, C.S.; Chuang, Y. *Jpn. J. Appl. Phys.* **1999**, *38*, L286–L288.
[16] Xu, Y.; Hu, Y.; Chen, Q.; Wen, J. *J. Mater. Chem.* **1995**, *5*, 219–221.
[17] Sekine, C.; Konya, N.; Minai, M.; Fujisawa, K. *Liq. Cryst.* **2001**, *28*, 1495–1503.
[18] Wu, S.T.; Hsu, C.S.; Shyu, K.F. *Appl. Phys. Lett.* **1999**, *74*, 344–346.
[19] Seed, A.J.; Toyne, K.J.; Goodby, J.W.; Hird, M. *J. Mater. Chem.* **2000**, *10*, 2069–2080.
[20] Liao, Y.M.; Chen, H.L.; Hsu, C.S.; Gauza, S.; Wu, S.T. *Liq. Cryst.* **2007**, *34*, 507–517.
[21] Sekine, C.; Konya, N.; Minai, M.; Fujisawa, K. *Liq. Cryst.* **2001**, *28*, 1361–1367.
[22] Sekine, C.; Ishitobi, M.; Iwakura, K.; Minai, M.; Fujisawa, K. *Liq. Cryst.* **2002**, *29*, 355–367.
[23] Lin, P.T.; Wu, S.T.; Chang, C.Y.; Hsu, C.S. *Mol. Cryst. Liq. Cryst.* **2004**, *411*, 1285–1295.
[24] Chang, C.Y.; Chien, S.Y.; Hsu, C.S.; Gauza, S.; Wu, S.T. *Liq. Cryst.* **2008**, *35*, 1–9.
[25] Catanescu, O.; Chien, L.C. *Liq. Cryst.* **2006**, *33*, 115–120.
[26] Wu, S.T.; Hsu, C.S.; Chuang, Y.Y.; Cheng, H.B. *Jpn. J. Appl. Phys.* **1999**, *39*, L38–L41.
[27] Yao, Y.H.; Kung, L.R.; Chang, S.W.; Hsu, C.S. *Liq. Cryst.* **2006**, *33*, 33–39.
[28] Li, H.F.; Wen, J.X. *Liq. Cryst.* **2006**, *33*, 1127–1131.
[29] Spells, D.J.; Lindsey, C.; Dalton, L.R.; Wu, S.T. *Liq. Cryst.* **2002**, *29*, 1529–1532.
[30] Hsu, C.S.; Shyu, K.F.; Chuang, Y.Y.; Wu, S.T. *Liq. Cryst.* **2000**, *27*, 283–287.
[31] Wu, S.T.; Hsu, C.S.; Chem, J.M. *Mol. Cryst. Liq. Cryst.* **1997**, *304*, 441–445.
[32] Wu, S.T.; Wu, C.S.; Warenghem, M.; Ismaili, M. *Opt. Eng.* **1993**, *32*, 1775–1780.
[33] Li, J.; Wu, S.T. *J. Appl. Phys.* **2004**, *95*, 896–901.
[34] Hsu, C.S.; Shyu, K.F.; Chuang, Y.Y.; *Liq. Cryst.* **2000**, *27*, 283–287.
[35] Yang, S.H.; Huang, C.H.; Chen, C.H.; Hsu, C.S. *Macromol. Chem. Phys.* **2009**, 210, 37–47.
[36] Wu, S.T.; Efron, U.; Hess L.D. *Appl. Opt.* **1984**, *23*, 3911–3915.
[37] Wu, S.T.; Wu, C.S. *Phys. Rev.* **1990**, *A42*, 2219–2227.
[38] Wu, S.T.; Lackner, A.M.; Efron, U. *Appl. Opt.* **1987**, *26*, 3441–3445.
[39] Maier, W.; Meier, G. *Z. Naturforsh, Teil A* **1961**, *16*, 262–267.
[40] Wen, C.H.; Fan, Y.H.; Wu, S.T.; Dabrowski, R.; Catanescu, C.O.; Chien, L.C. *Proc. SPIE*, **2002**, *4658*, 28–33.
[41] Wu, S.T. *Phys. Rev.* **1986**, A*33*, 1270–1274.
[42] Wu, S.T. *J. Appl. Phys.* **1991**, *69*, 2080–2087.
[43] Born, M.; Wolf, E. *Principles of Optics*; Pergamon Press: New York, 1980.
[44] Wu, S.T.; Ramos, E.; Finkenzeller, U. *J. Appl. Phys.* **1990**, 68, 78–85.
[45] Gauza, S.; Wang, H.Y.; Wen, C.H.; Wu, S.T.; Seed, A.J.; Dabrowski, R. *Jpn. J. Appl. Phys.* **2003**, *42*, 3463–3466.